Original Research

Evaluating eDNA and eRNA metabarcoding for aquatic biodiversity assessment: From bacteria to vertebrates

Yan Zhang [a, b, c], Yu Qiu [a], Kai Liu [d], Wenjun Zhong [a], Jianghua Yang [a], Florian Altermatt [b, c], Xiaowei Zhang [a, *]

[a] State Key Laboratory of Pollution Control J   Resource Reuse, School of the Environment, Nanjing University, Nanjing, 210023, China
[b] Department of Evolutionary Biology and Environmental Studies, University of Zurich, Zürich, Switzerland
[c] Department of Aquatic Ecology, Eawag: Swiss Federal Institute of Aquatic Science and Technology, Dübendorf, Switzerland
[d] Key Laboratory of Freshwater Fisheries and Germplasm Resources Utilization, Ministry of Agriculture and Rural Affairs, Freshwater Fisheries Research Center, Chinese Academy of Fishery Sciences, Wuxi, 214081, China

ARTICLE INFO

ABSTRACT

The monitoring and management of aquatic ecosystems depend on precise estimates of biodiversity. Metabarcoding analyses of environmental nucleic acids (eNAs), including environmental DNA (eDNA) and environmental RNA (eRNA), have garnered attention for their cost-effective and non-invasive biomonitoring capabilities. However, the accuracy of biodiversity estimates obtained through eNAs can vary among different organismal groups. Here we evaluate the performance of eDNA and eRNA metabarcoding across nine organismal groups, ranging from bacteria to terrestrial vertebrates, in three cross-sections of the Yangtze River, China. We observe robust complementarity between eDNA and eRNA data. The relative detectability of eNAs was notably influenced by major taxonomic groups and organismal sizes, with eDNA providing more robust signals for larger organisms. Both eDNA and eRNA exhibited similar cross-sectional and longitudinal patterns. However, the detectability of larger organisms declined in eRNA metabarcoding, possibly due to differential RNA release and decay among different organismal groups or sizes. While underscoring the potential of eDNA and eRNA in large river biomonitoring, we emphasize the need for differential interpretation of eDNA versus eRNA data. This highlights the importance of careful method selection and interpretation in biomonitoring studies.

1. Introduction

Freshwater, particularly riverine ecosystems, is experiencing a concerning decline in biodiversity [1]. This decline has prompted the emergence of the "Kunming-Montreal Global Biodiversity Framework," which underscores the need for innovative biomonitoring approaches to bolster conservation efforts and enhance environmental management [2]. Complete taxonomic groups (from bacteria to fishes) and their multiple organization levels (from population to food web) all contribute to the functions and stability of the aquatic ecosystem and, thus, should be monitored conclusively [3,4]. These new monitoring demands cannot be met by morphology-based biomonitoring methods alone, and there is an urgent need for reliable methods capable of detecting diverse taxonomic groups to ensure accurate biodiversity assessments [5,6].

The advent of environmental (e)DNA and environmental (e)RNA methods, collectively referred to as environmental nucleic acids (eNAs), has revolutionized the monitoring of numerous organismal groups in a rapid and non-invasive way. eDNA has emerged as a promising tool for biomonitoring, enhancing the detectability of target organisms [7] and enabling the retrieval of multiple organismal groups from a single sample [3,8]. However, due to its relative stability, eDNA integrates genetic signals across space and time [9,10]. While this is beneficial for upscaling biodiversity estimates to the catchment or landscape scale [10–12], it can impede discrimination at finer scales. Recently, there has been growing interest in exploring the potential application of eRNA in biodiversity surveys, given its faster production and turnover than eDNA [13,14]. Unlike eDNA, eRNA offers a more contemporary and

* Corresponding author.
E-mail address: zhangxw@nju.edu.cn (X. Zhang).

localized perspective [14,15], potentially being closely associated with the expression of functional genes and thereby offering insights into ecosystem functions rather than just states [16,17].

To fully exploit the potential of eNAs and understand where eDNA might fall short, it is essential to investigate the differences in species detectability between eDNA and eRNA [15]. Existing studies have produced mixed results, showing variation in the comparison of species detectability and community compositions using eDNA and eRNA [18−20]. These studies generally reported either a strong connection between eDNA- and eRNA-derived communities [19,21,22] or notable differences [18,23,24]. Typically, eDNA tended to exhibit higher alpha diversity but was also associated with higher false positive rates [20,25], with some exceptions (e.g., higher macroinvertebrate alpha diversity in eRNA in Ref. [26]). Additionally, specific taxa unique to eRNA have been observed in several studies [26,27].

These variations have given rise to hypotheses related to the "ecology of eNAs" (production, transportation, degradation, etc.), which could be influenced by various factors [28]. Organismal size is often closely related to the state of acquired eNAs. In the case of micro-organisms, it is possible the capture the whole individual organism, while in macro-organisms (e.g., fishes), it is only possible to acquire extracellular eNAs or inactive tissue samples [29]. Therefore, the relative detectability of eNAs, laying the groundwork for producing diverse biodiversity estimates and community compositions, might be associated with organismal size. Additionally, spatial scales, which are related to the degradation and transport of eNAs, can also contribute to variations in eNA comparisons [11]. Greater consistency in community structures derived from eDNA and eRNA samples might manifest in larger spatial scales with more distinct community structures.

Here, we employed a spatially nested sampling approach across multiple vertical layers and horizontal positions in three cross-sections upstream of the Yangtze River estuary to compare eDNA and eRNA results (Fig. 1). This area hosts diverse and abundant organisms, from microbes to fishes. The sheer size of the cross-sections and changes in water flow and salinity along the river offer potential insights into cross-sectional and longitudinal biodiversity gradients (see "Study Area" in the Supplementary Material). Nine taxonomic groups with different body sizes were retrieved to (1) assess the congruence and complementarity of eDNA and eRNA samples in detecting multiple organismal groups, (2) evaluate the relative detectability of eDNA and eRNA, and (3) compare the community structures of different organismal groups across eNA types and spatial scales.

2. Methods and materials

2.1. eNA sampling

Water samples were collected from three cross-sections (CS01, CS02, and CS03) upstream of the Yangtze estuary (a river stretch of 433 km in length) in June 2021 (Fig. 1, Supplementary Material Table S1). These cross-sections were over 1 km wide (1.32−2.48 km) and had an average depth of ~20 m (5.5−62.5 m), resulting in heterogeneous cross-sectional distribution patterns of organisms [30,31]. In each cross-section, two replicates of 1 L water were filtered on-site through Millipore 0.45 μm hydrophilic nylon membranes (Merck Millipore, USA) from nine sampling points distributed in three vertical layers and three horizontal locations. Two 1 L samples of tap water were filtered as the blank controls. Finally, 56 water samples were transported and stored at −80 °C (Supplementary Material Table S1). Please see "eNA Sampling" section in the Supplementary Material for details.

2.2. eNA extraction, polymerase chain reaction (PCR), and sequencing

To prevent contamination from exogenous eDNA/eRNA, nuclease-free water was used as blank control during the eNA extraction, reverse transcription and PCR processes. eDNA and eRNA were co-extracted from the 56 water samples by ZymoBIO-MICS™ DNA/RNA Mini Kit following standard manufacturer's procedures. The eNAs' quantity and quality were checked by Qubit 2.0 Fluorometer (Thermo Fisher Scientific) using Invitrogen™ Qubit™ 1X dsDNA HS Assay-Kits. eRNA samples were reversed into cDNA using HiScript III 1st Strand cDNA Synthesis Kit (Nanjing Vazyme Biotech Co. Ltd.). All samples were stored at −20 °C until the subsequent analysis.

The eNA samples were amplified using specific markers (Supplementary Material Table S2). The mitochondrial 16S V3 marker (~180 bp) was used to amplify prokaryote DNA (referred to as 16S) [32], the mitochondrial 18S V9 marker (~130 bp) was used to amplify micro-eukaryote DNA (referred to as 18S) [33], the mitochondrial cytochrome oxidase I marker (313 bp) was used to amplify metazoan DNA (referred to as COI) [34], and the mitochondrial 12S marker (167 bp) was used to amplify vertebrate DNA (referred to as 12S) [35]. Unique 12-bp nucleotide fragments (barcodes) were added to the 5′-ends of the forward or reverse primers (Shanghai Generay Biotech Co. Ltd).

For each sample, including negative controls of the eNA extraction and eRNA reverse transcription, three replicates of PCR were performed in a 30 μL reaction mixture. The reaction mixture consisted of 19.1 μL of ddH$_2$O, 6 μL of 5 × Phusion Green HF Buffer, 0.6 μL of 10 mM dNTPs, 1 μL of 10 μM forward and reverse primers, 2 μL of the template, and 0.3 μL of Phusion Green Hot Start II High-Fidelity DNA Polymerase from Thermo Fisher Scientific. The amplification protocol included an initial denaturation at 98 °C for 30 s, followed by 30 cycles of denaturation at 98 °C for 5 s, annealing at the appropriate annealing temperature (T$_m$, Supplementary Material Table S2) for 30 s, and extension at 72 °C for 15 s. A final extension step was performed at 72 °C for 5 min. After the PCR assays, the products were cooled to 4 °C. Two PCR-negative controls were included using nuclease-free water as the DNA template. The PCR products for all eNA samples and negative controls were checked using a 2% agarose gel and combined in equal volumes. Libraries were constructed with distinct adaptors
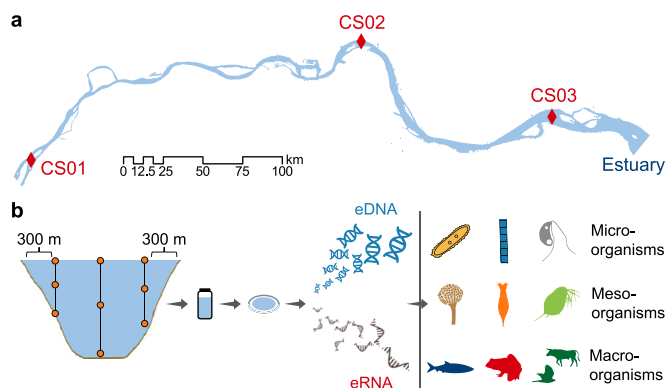

Fig. 1. Design of sampling and eNAs metabarcoding in the Yangtze River. a, Location of cross-sections sampled. **b,** Two 1-Liter water samples were taken from nine sampling points within three cross-sections (CS01/02/03). Environmental (e)DNA and environmental (e)RNA were separated and extracted from the paired samples to retrieve nine organismal groups with different body sizes. The shapefile of the Yangtze River was extracted from GLCF: Landsat Global Inland Water in Google Earth Engine ("GLCF/GLS_WATER"), and the map was plotted in ArcGIS 10.7.

using the VAHTS Universal DNA Library Prep Kit for Illumina (Vazyme, China). All libraries were sequenced in the NovaSeq 6000 platform (Illumina, Inc., US). An additional 5% of PhiX (control DNA) was added to the library prior to sequencing. All wet-lab experiments were conducted under a sterile bench that underwent ultraviolet (UV) light cleaning for half an hour before use to minimize the risk of contamination.

2.3. Bioinformatics

The raw data were processed using the SWARM algorithm [36]. First, the paired-end reads obtained from the NOVA instrument were assembled using VSEARCH (2.14.1) [37]. The samples were then demultiplexed, and adaptors and primers were trimmed using the CUTADAPT program [38]. For demultiplexing, a tolerance of three mismatches was allowed in tags, while sequences containing ambiguous nucleotides were discarded. Next, unsupervised clustering was performed with SWARM, employing a minimum distance of one nucleotide between each amplicon sequence variant (ASV). Thirdly, we used the ecotag algorithm to assign taxonomic labels to all ASVs. This algorithm relies on the NCBI phylogenetic tree and follows a lowest common ancestor (LCA) approach using the OBITools toolkit. Additionally, we carefully curated the database against the European Nucleotide Archive for each primer used following the instructions in Ref. [39]. Following that, ASVs with less than ten reads or those that were deemed too short or too long (16S: 150−250 bp, 18S: 130−230 bp, COI: 250−400 bp, Tele02: 150−220 bp) were excluded. Finally, the LULU algorithm was used to identify and remove erroneous ASVs based on sequence identity, abundance, and co-occurrence patterns [40].

Before downstream analysis, "contaminated" ASVs were identified using a prevalence-based test with a probability threshold of 0.5, employing the *isContaminant*() function from the "decontam" R package [41]. All replicates of each sample were combined, and samples with a sequencing depth of no more than 10,000 were discarded. The remaining samples were rarefied to the lowest sequencing depth using the *rrarefy*() function from the "vegan" package [42]. To prioritize robust detections over the noise, only ASVs with a total abundance greater than 0.1% were retained for further analysis.

2.4. Categories of organisms

We generated rarefaction curves for each primer using the *incidence_fre* option of the "iNEXT" package, which is recommended for analyzing incidence data (presence/absence of species) [43]. The ASVs were then categorized into nine taxonomic groups: 16S ASVs were assigned to bacteria; 18S ASVs were assigned to algae, protozoa, and fungi; COI ASVs were assigned to Rotifera and Arthropoda; and 12S ASVs were assigned to fish, amphibians, and terrestrial vertebrates (birds and mammals). Based on their average body lengths (defined as the mean body lengths at the family level, Supplementary Material Table S3), these taxonomic groups were further grouped into micro-organisms (bacteria, algae, and protozoa), meso-organisms (fungi, Rotifera, and Arthropoda), and macro-organisms (fish, amphibians, and terrestrial vertebrates). Taxa of the nine taxonomic groups were defined at the family level for bacteria, fungi, amphibians, and genus for the others.

2.5. Statistics

ASVs/taxa captured by eNAs. Paired *t*-tests were performed to compare ASV/taxa richness between eDNA and eRNA [44]. Analysis of Variance (ANOVA) was employed to analyze differences in alpha diversity between cross-sections [45]. Linear mixed models with

cross-section as a random factor were used to explore differences across vertical layers and horizontal locations within cross-sections [46]. Please see the "Equations of Group Comparison" section in the Supplementary Material for the detailed models.

To validate the detectability of eDNA and eRNA, we compared the results of eNAs with morphology-based fish monitoring data and historical records of fish species in the downstream Yangtze River [47]. Although it would be advantageous to compare the eDNA/eRNA data with morphology-based biomonitoring data across diverse taxonomic groups, fish represent the sole group for which we could gather morphology data in this study. The conventional fish monitoring data on morphology-based method was obtained from the "Yangtze Fisheries Resources and Environment Investigation Project" conducted between 2017 and 2021. Fish occurrence data from three cross-sections during the same period were extracted. Please refer to Ref. [48] for the detailed monitoring method. The mismatches between eNAs and morphological results, partly attributed to spatial aggregation and decay of eNAs, were illustrated using "false positives" and "false negatives" [49]. Specifically, false positives were defined as the genera of fish detected in eNAs but not in the morphological results, while false negatives were defined as the genera of fish not detected in eNAs but detected in the morphological results. The false positive and false negative rates were further defined as the proportion of false positives or false negatives to the total number of fish genera detected in eNAs. Paired *t*-tests were used to compare the false positive and false negative rates between eDNA and eRNA [44].

Relative detectability of eNAs. We used the number of ASVs and taxa to show the gamma and alpha diversity patterns. The proportion of overlapped ASVs/taxa (*Overlapped α*) and the richness ratio of eDNA to eRNA (*α detected ratio*) were used to assess the congruence and relative detectability of the nine taxonomic groups, according to equations (1) and (2): *N* is the number of ASVs or taxa.

$$\alpha\ detected\ ratio = \frac{N_{eDNA}}{N_{eRNA}} \tag{1}$$

$$Overlapped\ \alpha = \frac{N_{eDNA \cap eRNA}}{N_{eDNA \cup eRNA}} \tag{2}$$

The effect of organismal size on the detectability of eNAs was investigated using a linear mixed model (LME), with the identity of the cross-section as a random factor [46]. Organismal sizes were logarithmically transformed using a base of ten.

Community compositions across organismal groups and spatial scales. Community compositions were visualized based on PCoA plots using the "vegan" R package [42]. We ran PERMANOVA tests to assess the differences between eNA types, vertical layers, horizontal locations, and cross-sections.

We then calculated the Jaccard dissimilarity indices for each taxonomic group to capture the beta diversity patterns. The pairwise dissimilarity matrix between samples was calculated and partitioned into turnover and nestedness components using the "betapart" R package [50]. The community variations in eDNA or eRNA were quantified as the Jaccard dissimilarities and their turnover and nestedness components between sampling points, either within the same cross-section (cross-sectional) or across different cross-sections (longitudinal). Paired *t*-tests were performed to compare community variations between eDNA and eRNA [44]. The ratios of Jaccard dissimilarities of eDNA compared to eRNA samples were calculated according to equation (3): $\beta - eDNA_{ij}$ or $\beta - eRNA_{ij}$ refers to the Jaccard dissimilarity or its components between sampling points *i* and *j*.
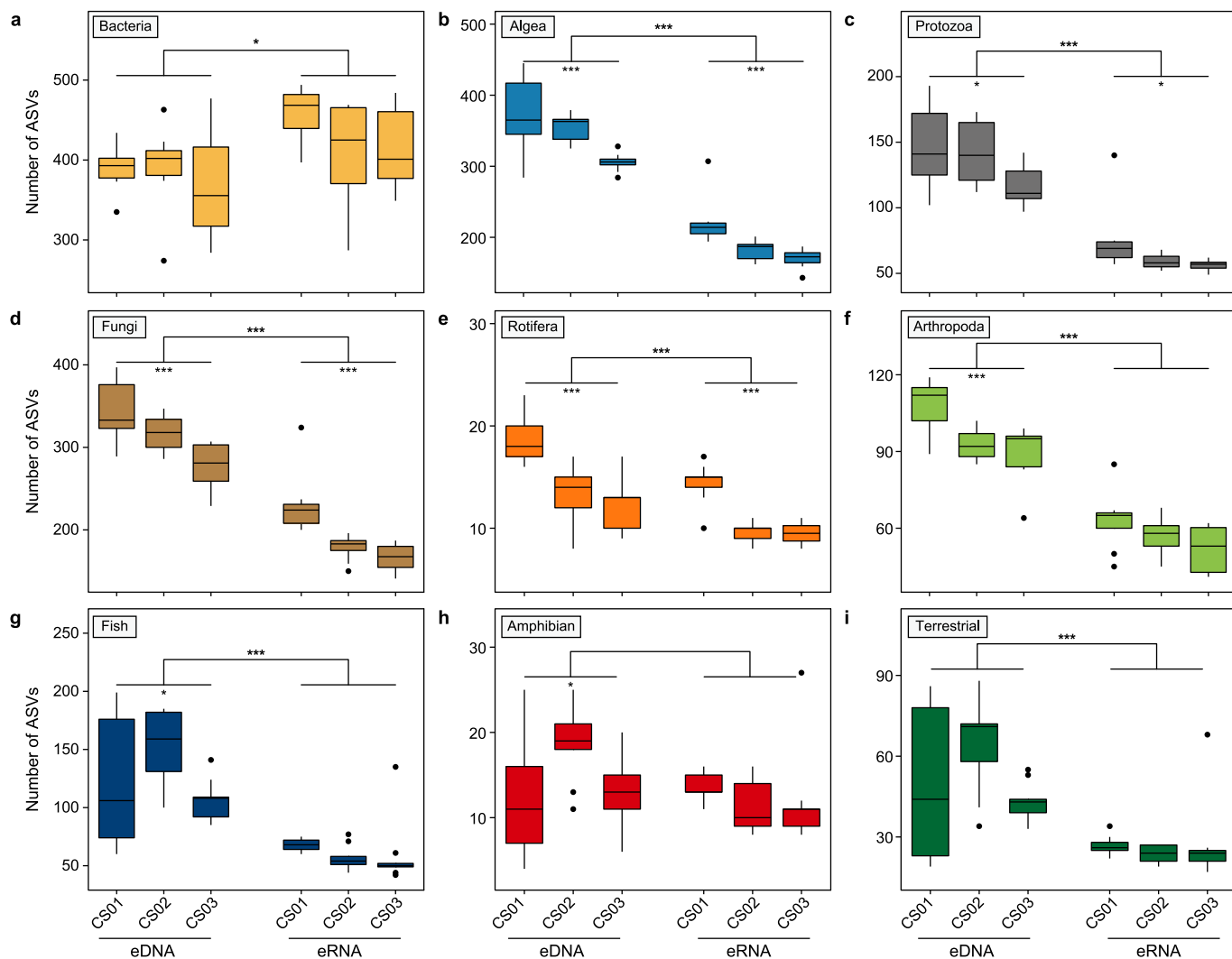
Fig. 2. ASV richness in cross-sections and eDNA/eRNA samples. The comparison of eDNA and eRNA samples was based on the paired *t*-tests, and that of cross-sections (CS01/02/03) was based on ANOVA. **a**, Bacteria; **b**, Algae; **c**, Protozoa; **d**, Fungi; **e**, Rotifera; **f**, Arthropoda; **g**, Fish; **h**, Amphibian; **i**, Terrestrial vertebrates. ***$p < 0.001$; **$p < 0.01$; *$p < 0.05$.

$$\beta \ ratio_{ij} = \frac{\beta - \text{eDNA}_{ij}}{\beta - \text{eRNA}_{ij}} \qquad (3)$$

Spatial scale effects on the ratios of Jaccard dissimilarities of eDNA compared to eRNA samples were examined using LME with organismal size as the random factor, while the effects of organismal sizes were analyzed using a generalized least square (GLS) linear model [46]. All analyses were conducted in R (version 4.0.5).

3. Results

3.1. Congruence and complementary of eNAs in capturing ASVs and taxa

eNA data were assigned to microorganisms (bacteria, algae, and protozoa), meso-organisms (fungi, Rotifera, and Arthropoda), and macroorganisms (fish, amphibians, and terrestrial vertebrates). For these groups, 1806; 1020; 448; 1027; 34; 212; 508; 83; and 313 ASVs were detected, respectively, assigned to 285 orders, 467 families, 718 genera, and 783 species (Supplementary Material Table S4). Details on bioinformatics are presented in the

"Summary of Bioinformatics" section in the Supplementary Material. Organisms exhibited consistent detection of abundant ASVs/taxa in both eDNA and eRNA samples, whereas rare ASVs/taxa detection showed variability. Between 18.85% and 80.19% of ASVs overlapped in eDNA and eRNA samples, accounting for 93.68% of total reads (Supplementary Material Figs. S1—S2). More than half of the ASVs (ranging from 53.93% for protozoa to 80.19% for Arthropoda) overlapped in micro- and meso-organisms, and only 18.85% (terrestrial vertebrates) to 32.48% (fish) in macro-organisms (Supplementary Material Fig. S1). Except for bacteria, Arthropoda, and amphibians, more ASVs were detected in eDNA samples. Notably, 35.78—65.45% of ASVs significantly differed between eNAs (Supplementary Material Table S5). At the taxa level, 73.68—100% were shared between the eNAs types, accounting for more than 99% of reads (Supplementary Material Figs. S1—S2).

Consistency of the ASV/taxa richness between eDNA and eRNA samples was evident in micro- and meso-organisms (excluding bacteria). The ASV richness monitored by eDNA and eRNA was remarkably consistent in algae, fungi, Rotifera, and Arthropoda. Still, no significant linear relationship was detected between the eNAs for macro-organisms (Fig. 3). No significant linear relationships were found at the taxa level except for protozoa
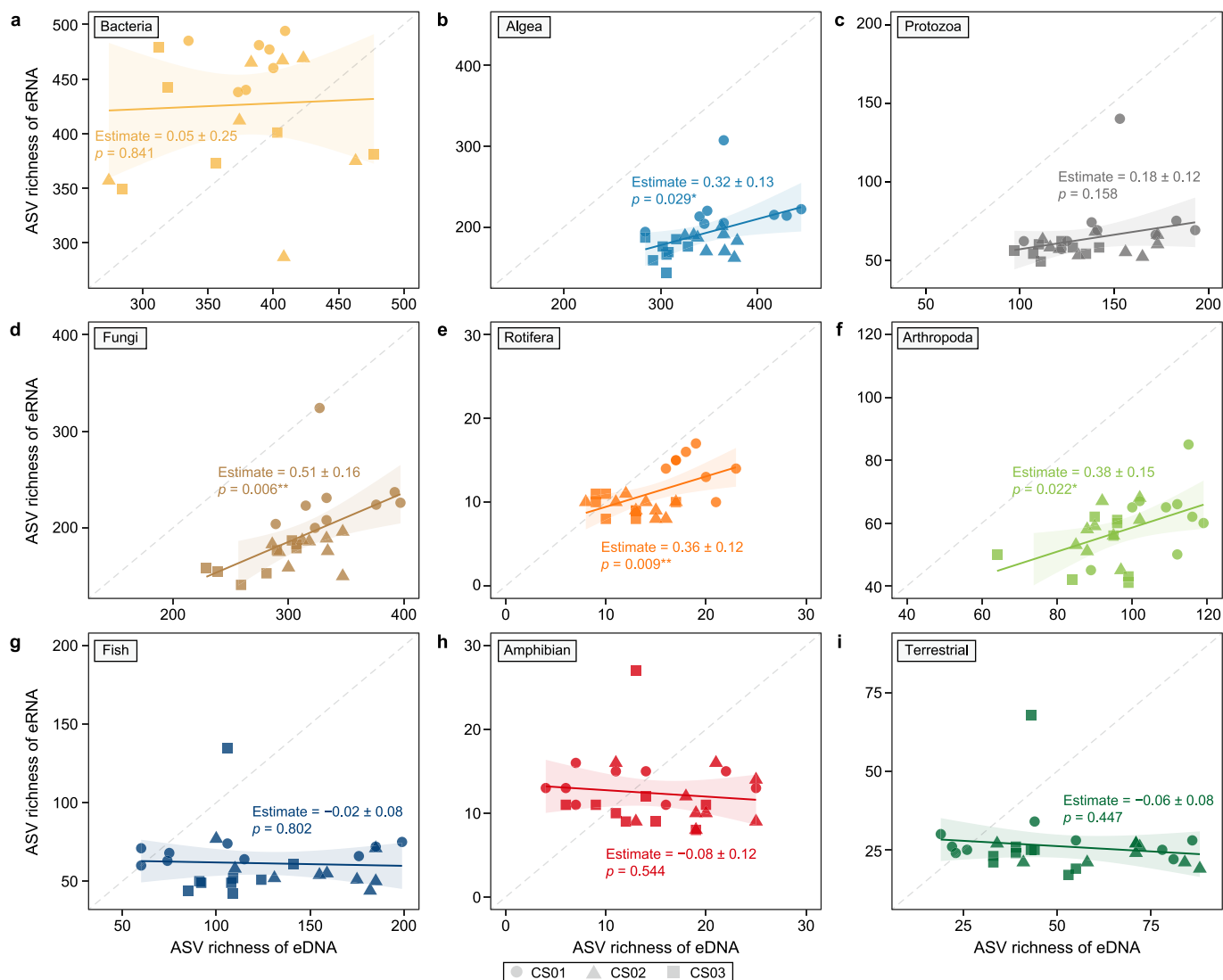
Fig. 3. Congruence of ASV richness between eDNA and eRNA samples. a, Bacteria; **b**, Algae; **c**, Protozoa; **d**, Fungi; **e**, Rotifera; **f**, Arthropoda; **g**, Fish; **h**, Amphibian; **i**, Terrestrial vertebrates. ***$p < 0.001$; **$p < 0.01$; *$p < 0.05$.

(Supplementary Material Fig. S5). ASV/taxa richness displayed insignificant cross-sectional patterns but exhibited significant longitudinal patterns in both eDNA and eRNA samples (Supplementary Material Table S7). No notable variations in alpha diversity for both eDNA and eRNA samples were observed among vertical layers or horizontal locations within cross-sections (Supplementary Material Table S7, LME $p > 0.05$). In contrast, eDNA samples exhibited stronger longitudinal trends among larger organisms, whereas eRNA samples demonstrated greater spatial discrimination among smaller organisms (Fig. 2; Supplementary Material Fig. S4, Table S7). More details can be found in the "Longitudinal Patterns of ASV/Taxa Richness" section of the Supplementary Material.

Specifically, we compared the fishes detected by eNAs with morphological data and historical records (Supplementary Material Fig. S3, Table S6). Fifteen genera (17.24%) were simultaneously observed by the eDNA, eRNA, and morphological methods, all of which had historical records. Another 46 genera (52.87%) were detected by both eDNA and eRNA methods, of which 32 (36.78%) genera had historical records. Additionally, ten genera (11.49%)

were detected only in eDNA samples. We obtained similar results when considering single cross-sections. Overall, the false positive rates of eDNA were slightly larger than those of eRNA, while the false negative rates were higher in eRNA (Supplementary Material Fig. S3, paired t-tests; False positive rate, $t_{26} = 3.17$, $p = 0.004$; False negative rate, $t_{26} = -4.17$, $p < 0.001$).

3.2. Effect of organismal size on the detectability of eNAs

eDNA samples revealed a higher number of ASVs and taxa, excluding bacteria. The detectability ratio of eDNA to eRNA increased with organism size, indicating stronger eDNA signals relative to eRNA for larger organisms. More bacteria ASVs were found in eRNA samples than eDNA samples (Fig. 2, Supplementary Material Table S7 paired t-test; $t_{19} = -2.85$, $p = 0.010$). For the other organisms, the number of ASVs in eDNA samples was significantly higher than in eRNA samples (Fig. 2; Supplementary Material Table S7). The α detected ratio at the ASV level increased significantly with the body size of organisms (Fig. 4, LME $p < 0.001$), and the proportion of overlapped α decreased (Fig. 4, LME $p < 0.001$). At
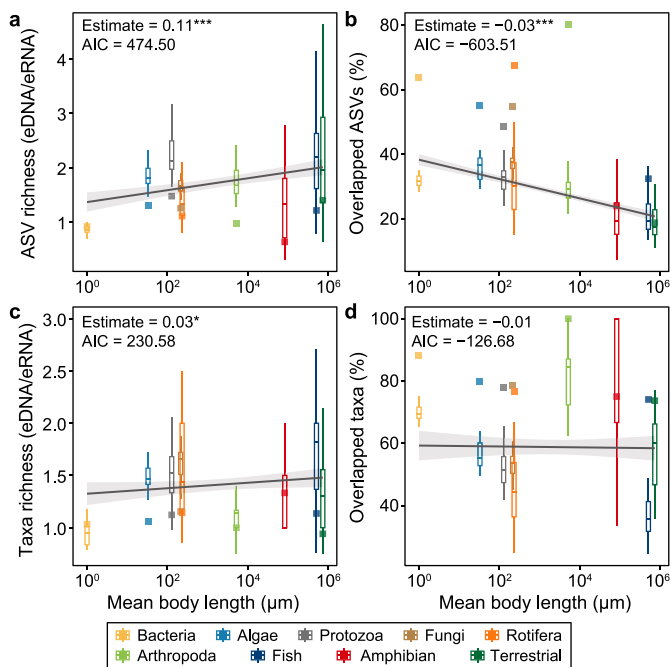
Fig. 4. Effects of Organismal Sizes on the Detectability of eNAs. a, c, The ASV (**a**) and Taxa (**c**) richness ratio in eDNA and eRNA samples. **b, d**, The proportion of overlapped ASVs (**b**) or taxa (**d**) in nine organism groups. The squares represent gamma diversity. Regressions were conducted by linear mixed models with the identity of cross-sections as the random factor. The grey envelope surrounding each line represents a 95% confidential interval. ***$p < 0.001$; **$p < 0.01$; *$p < 0.05$.

the taxa level, eRNA samples revealed more bacterial taxa than eDNA samples (Supplementary Material Fig. S4, Table S7 paired *t*-test; $t_{19} = -2.28$, $p = 0.034$). In contrast, for all the other organisms, the number of taxa detected in eDNA samples was significantly greater than in eRNA samples (Supplementary Material Fig. S4, Table S7). The α detected ratio increased significantly with the body size of organisms (Fig. 4, LME $p = 0.015$), while no significant relationships were found in the proportion of overlapped α (Fig. 4, LME $p = 0.155$).

3.3. Community structures in eNAs across organismal groups and spatial scales

The community structures detected by eDNA and eRNA exhibited significant differences for all nine organismal groups, as measured using Jaccard dissimilarities, and these variations were greater than the spatial differences observed within the eDNA/eRNA samples themselves (Fig. 5, Supplementary Material Table S8). Significant differences in community structure were found among horizontal locations for algae, protozoa, Rotifera, amphibians, and terrestrial vertebrates in both eDNA and eRNA samples. All organismal groups except bacteria had distinct community structures across cross-sections when assessed using eDNA and eRNA samples (Supplementary Material Table S8). In the case of eRNA samples, elevated turnover components were noted across most organismal groups, while eDNA samples displayed higher nestedness values compared to eRNA samples (Supplementary Material Fig. S6). Details can be found in the "Turnover and Nestedness Components" section of the Supplementary Material.
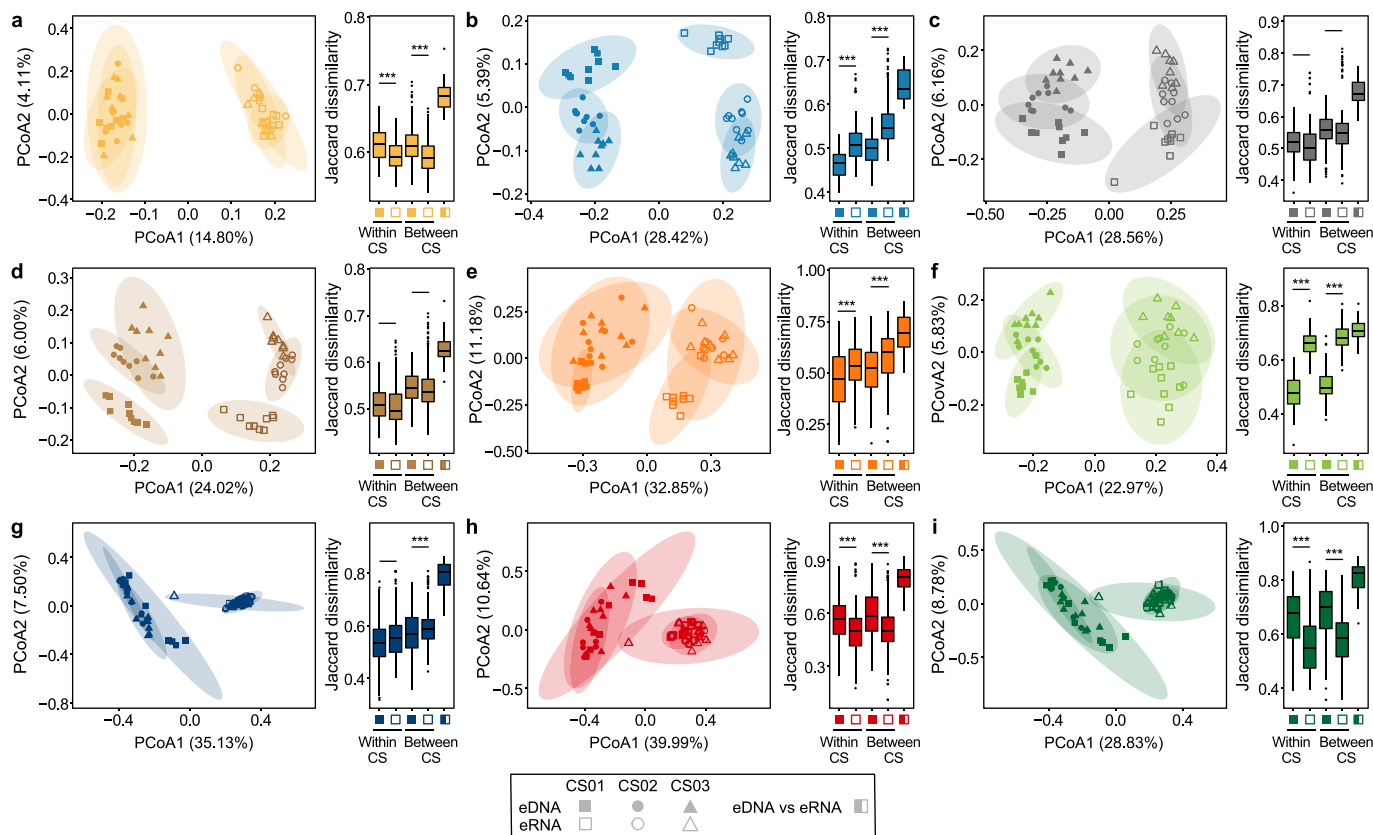

Fig. 5. PCoA plots of aquatic communities in the three cross-sections (CS01/02/03) from the Yangtze River based on Jaccard dissimilarities. a, Bacteria; **b**, Algae; **c**, Protozoa; **d**, Fungi; **e**, Rotifera; **f**, Arthropoda; **g**, Fish; **h**, Amphibian; **i**, Terrestrial vertebrates. The left panel illustrated the PCoA plot. Different shapes represented three cross-sections, with eDNA solid and eRNA hollow. The right panel described Jaccard dissimilarities between eDNA and eRNA and within or between cross-sections. The comparison of eDNA and eRNA samples was based on paired *t*-tests. ***$p < 0.001$; **$p < 0.01$; *$p < 0.05$.

For both cross-sectional and longitudinal scales, the eDNA samples exhibited higher overall Jaccard dissimilarities for bacteria, amphibians, and terrestrial vertebrates, while the eRNA samples showed higher dissimilarities for algae, Rotifera, Arthropoda, and fish. No significant differences were observed in the protozoa and fungi (Fig. 5). eRNA samples exhibited higher turnover components across most organismal groups, whereas eDNA samples displayed higher nestedness components (Supplementary Material Fig. S6). Details can be found in the "Comparison of Community Variations in eNA" section of the Supplementary Material.

The ratios of community variations of eDNA to eRNA samples increased with organism size and remained consistent across both spatial scales (Supplementary Material Fig. S7, Table S9). Linear mixed models showed no significant effect of spatial scales on the ratios of Jaccard dissimilarities between eDNA and eRNA, nor on turnover and nestedness components (Supplementary Material Table S9, LME $p > 0.05$). Based on total Jaccard dissimilarity, the ratios of eDNA to eRNA community variations significantly increased with organism size (Supplementary Material Fig. S7; cross-sectional LME $p < 0.001$, longitudinal GLS $p < 0.001$). Nestedness components showed trends similar to total Jaccard dissimilarities (Supplementary Material Table S9). Longitudinal turnover components decreased as organism size increased, while cross-sectional turnover components had no significant relationship (Supplementary Material Table S9).

4. Discussion

Using both eDNA and eRNA-based data upstream of the Yangtze estuary, we provided systematic insights into the detectability of multiple organismal groups by eDNA and eRNA. Our results indicated that eDNA and eRNA data exhibit strong complementarity yet vary among different organismal groups. The relative detectability of eDNA and eRNA was significantly affected by organismal size and across organismal groups, with a relatively higher signal for eDNA for larger organisms. Both eDNA and eRNA yielded similar cross-sectional and longitudinal spatial distribution patterns. The lower detectability of large organisms by eRNA indicates that eDNA is differentially and spatially integrated at smaller scales. Our work confirmed the complementarity of eDNA and eRNA in monitoring multiple aquatic organismal groups, emphasizing the importance of organismal size in method selection and interpretation of eNA results.

We found strong yet distinct complementarity between eDNA and eRNA data in monitoring various aquatic organismal groups. Both eDNA and eRNA performed similarly in the detection of abundant ASVs/taxa, with ASV overlaps ranging from 18.85% to 80.19% (Supplementary Material Fig. S1). Micro- and meso-organisms showed substantial ASV overlaps between eDNA and eRNA, while in macro-organisms, the overlaps were lower, varying from 18.85% to 32.48%. The consistency in ASV/taxa richness was evident in micro- and meso-organisms, except for bacteria, where eDNA consistently identified more ASVs/taxa (Fig. 3). In the context of current comparative biomonitoring studies employing both eDNA and eRNA, eRNA was preferred for monitoring "active" communities [10,51,52], due to its higher productivity [53] and reduced susceptibility to terrestrial and upstream error signals [54]. The lower number of terrestrial vertebrate ASVs in eRNA suggested diminished terrestrial genetic material influence in our analysis (Fig. 2). However, the rapid conversion of eRNA may have led to a potential underestimation of biodiversity [51], especially in larger organisms. In summary, eDNA and eRNA could effectively monitor diverse yet complementary aquatic organisms, but caution is needed when interpreting data for larger organisms using eRNA.

A significant positive relationship was observed in the detection of eNAs concerning organismal size, with eDNA being relatively more detected versus eRNA (Fig. 4). The variations in eNA detectability are likely influenced by multiple factors primarily associated with the "ecology of eNAs" [28]. Previous research has identified differences in eRNA degradation rates across various organismal groups, contrasting with the stable degradation rates of eDNA, and that the spatial and temporal integration of eDNA vs. eRNA is different [51]. In particular, the latter (eRNA) may be a more local and more contemporary signal. Additionally, environmental variables such as temperature [52], pH [55], genetic origins [56], and the physiological characteristics of the source organisms [16] can impact the interpretation of eNA data. Furthermore, organismal size, potentially associated with different physiology, behavior, or trophic levels [57], could affect the release (and ultimately the detection) of DNA versus RNA [58]. The size-based differences in relative detectability may need to be considered, particularly in constructing meta-webs using eNAs [59].

Both eDNA and eRNA yielded similar cross-sectional and longitudinal spatial distribution patterns. However, a spatially and temporally more confined detectability of eRNA indicates that larger organisms, often found at lower densities and spatially more scattered, will be less likely to be detected locally. Notably, eDNA and eRNA revealed distinctive community structures that consistently exceeded spatial variations across all nine organismal groups (Fig. 5), aligning with prior research [24,26]. While eRNA is generally recognized for its greater spatial discriminative capabilities [27] and stronger correlation with environmental parameters [23], there are exceptions, such as instances where eRNA identified less spatial differences in metazoan populations due to reduced species richness [60]. Furthermore, our findings underscored a significant increase in the ratio of spatial community variations between eDNA and eRNA as organismal size increased (Supplementary Material Fig. S7). As a result, while eRNA excels in detecting subtle spatial disparities among smaller organisms, its limited ability to detect larger organisms may lead to the loss of critical spatial information.

5. Conclusion

Our results indicated that eDNA and eRNA data exhibit strong complementarity for detecting taxa, yet the strength of this complementarity/consistency varied among different organismal groups. The relative detectability of eDNA and eRNA was significantly affected by organismal size and across organismal groups, with a relatively higher signal for eDNA for larger organisms. Both eDNA and eRNA yielded similar cross-sectional and longitudinal spatial distribution patterns. The lower detectability of large organisms by eRNA indicates that eDNA is differentially and spatially integrated at smaller scales. These findings could contribute to the growing body of knowledge on applying eNAs in biomonitoring and underscore the importance of thoughtful method selection and interpretation in this field.

CRediT authorship contribution statement

Yan Zhang: Writing - Original Draft, Visualization, Validation, Software, Resources, Methodology, Investigation, Formal Analysis, Data Curation, Conceptualization. **Yu Qiu:** Investigation, Formal Analysis, Data Curation. **Kai Liu:** Resources, Data Curation. **Wenjun Zhong:** Methodology, Investigation. **Jianghua Yang:** Writing - Review & Editing. **Florian Altermatt:** Writing - Review & Editing, Supervision, Conceptualization. **Xiaowei Zhang:** Writing - Review & Editing, Validation, Supervision, Funding Acquisition, Conceptualization.

Declaration of competing interest

The authors declare that they have no known competing financial interests or personal relationships that could have appeared to influence the work reported in this paper.

Acknowledgments

Appendix A. Supplementary data

Supplementary data to this article can be found online at https://doi.org/10.1016/j.ese.2024.100441.

References

[1] E.S. Brondizio, et al., Global Assessment Report on Biodiversity and Ecosystem Services of the Intergovernmental Science-Policy Platform on Biodiversity and Ecosystem Services, 2019.
[2] E. Nicholson, et al., Scientific foundations for an ecosystem goal, milestones and indicators for the post-2020 global biodiversity framework, Nature Ecology & Evolution 5 (10) (2021) 1338–1349.
[3] F. Li, et al., Human activities' fingerprint on multitrophic biodiversity and ecosystem functions across a major river catchment in China, Global Change Biol. 26 (12) (2020) 6867–6879.
[4] F. Li, et al., Destabilizing effects of environmental stressors on aquatic communities and interaction networks across a major river basin, Environ. Sci. Technol. 57 (20) (2023) 7828–7839.
[5] D.J. Baird, M. Hajibabaei, Biomonitoring 2.0: a new paradigm in ecosystem assessment made possible by next-generation DNA sequencing, Mol. Ecol. 21 (2012) 2039–2044.
[6] X. Zhang, Environmental DNA shaping A new era of ecotoxicological research, Environ. Sci. Technol. 53 (10) (2019) 5605–5613.
[7] F. Keck, et al., Meta-analysis shows both congruence and complementarity of DNA and eDNA metabarcoding to traditional methods for biological community assessment, Mol. Ecol. 31 (6) (2022) 1820–1835.
[8] Y. Zhang, et al., Holistic pelagic biodiversity monitoring of the Black Sea via eDNA metabarcoding approach: from bacteria to marine mammals, Environ. Int. 135 (2020) 105307.
[9] J.J. Eichmiller, S.E. Best, P.W. Sorensen, Effects of temperature and trophic state on degradation of environmental DNA in lake water, Environ. Sci. Technol. 50 (4) (2016) 1859–1867.
[10] K. Deiner, et al., Environmental DNA reveals that rivers are conveyer belts of biodiversity information, Nat. Commun. 7 (2016) 12544.
[11] L. Carraro, et al., Environmental DNA allows upscaling spatial patterns of biodiversity in freshwater ecosystems, Nat. Commun. 11 (1) (2020) 3585.
[12] L. Carraro, J.B. Stauffer, F. Altermatt, How to design optimal eDNA sampling strategies for biomonitoring in river networks, Environmental DNA 3 (1) (2020) 157–172.
[13] H.D. Veilleux, M.D. Misutka, C.N. Glover, Environmental DNA and environmental RNA: current and prospective applications for biological monitoring, Sci. Total Environ. 782 (2021) 146891.
[14] M.C. Yates, A.M. Derry, M.E. Cristescu, Environmental RNA: a revolution in ecological resolution? Trends Ecol. Evol. 36 (7) (2021) 601–609.
[15] M.E. Cristescu, Can environmental RNA revolutionize biodiversity science? Trends Ecol. Evol. 34 (8) (2019) 694–697.
[16] M.B. Parsley, C.S. Goldberg, Environmental RNA can distinguish life stages in amphibian populations, Molecular Ecology Resources (2023) 1–9.
[17] K. Tsuri, et al., Messenger RNA typing of environmental RNA (eRNA): a case study on zebrafish tank water with perspectives for the future development of eRNA analysis on aquatic vertebrates, Environmental DNA 3 (1) (2020) 14–21.
[18] M. Adamo, et al., Metabarcoding on both environmental DNA and RNA highlights differences between fungal communities sampled in different habitats, PLoS One 15 (12) (2020) e0244682.
[19] J.E. Littlefair, M.D. Rennie, M.E. Cristescu, Environmental nucleic acids: a field-based comparison for monitoring freshwater habitats using eDNA and eRNA, Molecular Ecology Resources 22 (8) (2022) 2928–2940.
[20] K. Miyata, et al., Fish environmental RNA enables precise ecological surveys with high positive predictivity, Ecol. Indicat. (2021) 128.
[21] K. Miyata, et al., Comparative environmental RNA and DNA metabarcoding analysis of river algae and arthropods for ecological surveys and water quality assessment, Sci. Rep. 12 (1) (2022) 19828.
[22] J.A. Visco, et al., Environmental monitoring: inferring the diatom index from next-generation sequencing data, Environ. Sci. Technol. 49 (13) (2015) 7597–7605.
[23] H. Kong, et al., RNA outperforms DNA-based metabarcoding in assessing the diversity and response of microeukaryotes to environmental variables in the Arctic Ocean, Sci. Total Environ. 876 (2023) 162608.
[24] F. Lejzerowicz, et al., Eukaryotic biodiversity and spatial patterns in the clarion-clipperton zone and other abyssal regions: insights from sediment DNA and RNA metabarcoding, Front. Mar. Sci. 8 (2021) 671033.
[25] U. von Ammon, et al., Linking environmental DNA and RNA for improved detection of the marine invasive fanworm sabella spallanzanii, Front. Mar. Sci. 6 (2019) 621.
[26] M.S. Giroux, et al., Environmental RNA as a tool for marine community biodiversity assessments, Sci. Rep. 12 (1) (2022) 17782.
[27] T. Kitahashi, et al., Meiofaunal diversity at a seamount in the pacific ocean: a comprehensive study using environmental DNA and RNA, Deep Sea Res. Oceanogr. Res. Pap. 160 (2020) 103253.
[28] M.C. Yates, et al., Beyond Species Detection—Leveraging Environmental DNA and Environmental RNA to Push beyond Presence/absence Applications, Environmental DNA, 2023, pp. 1–7.
[29] M. Yao, et al., Fishing for fish environmental DNA: ecological applications, methodological considerations, surveying designs, and ways forward, Mol. Ecol. 31 (20) (2022) 5132–5164.
[30] F. Altermatt, et al., Quantifying biodiversity using eDNA from water bodies: general principles and recommendations for sampling designs, Environmental DNA (2023) 1–12, 00.
[31] Y. Zhang, et al., Fishing eDNA in one of the world's largest rivers: a case study of cross-sectional and depth profile sampling in the Yangtze, Environ. Sci. Technol. 57 (51) (2023) 21691–21703.
[32] A. Klindworth, et al., Evaluation of general 16S ribosomal RNA gene PCR primers for classical and next-generation sequencing-based diversity studies, Nucleic Acids Res. 41 (1) (2013) e1.
[33] S. Malviya, et al., Insights into global diatom distribution and diversity in the world's ocean, Proc. Natl. Acad. Sci. USA 113 (11) (2016) E1516–E1525.
[34] J. Geller, et al., Redesign of PCR primers for mitochondrial cytochrome c oxidase subunit I for marine invertebrates and application in all-taxa biotic surveys, Molecular Ecology Resources 13 (5) (2013) 851–861.
[35] P. Taberlet, et al., Environmental DNA: for Biodiversity Research and Monitoring, Oxford University Press, 2018.
[36] V. Marques, et al., Blind assessment of vertebrate taxonomic diversity across spatial scales by clustering environmental DNA metabarcoding sequences, Ecography 43 (12) (2020) 1779–1790.
[37] T. Rognes, et al., VSEARCH: a versatile open source tool for metagenomics, PeerJ 4 (2016) e2584.
[38] M. Martin, Cutadapt removes adapter sequences from high-throughput sequencing reads, EMBnet.journal 17 (2011) 10–12.
[39] F. Boyer, et al., OBITOOLS: a UNIX-inspired software package for DNA metabarcoding, Molecular Ecology Resources 16 (1) (2016) 176–182.
[40] T.G. Frøslev, et al., Algorithm for post-clustering curation of DNA amplicon data yields reliable biodiversity estimates, Nat. Commun. 8 (1) (2017) 1188.
[41] N.M. Davis, et al., Simple statistical identification and removal of contaminant sequences in marker-gene and metagenomics data, Microbiome 6 (1) (2018) 226.
[42] P. Dixon, VEGAN, a package of R functions for community ecology, J. Veg. Sci. 14 (6) (2003) 927–930.
[43] T.C. Hsieh, et al., iNEXT: an R package for rarefaction and extrapolation of species diversity (Hill numbers), Methods Ecol. Evol. 7 (12) (2016) 1451–1456.
[44] H. Hsu, P.A. Lachenbruch, Paired T Test, Wiley StatsRef: Statistics Reference Online, 2014.
[45] L. St, S. Wold, Analysis of variance (ANOVA), Chemometr. Intell. Lab. Syst. 6 (4) (1989) 259–272.
[46] J. Pinheiro, et al., Nlme: linear and nonlinear mixed effects models, R package version 31-110 3 (2013) 1–113.
[47] Y. Shen, et al., DNA barcoding the ichthyofauna of the Yangtze River: insights from the molecular inventory of a mega-diverse temperate fauna, Molecular Ecology Resources 19 (5) (2018) 1278–1291.
[48] H. Yang, et al., Status of aquatic organisms resources and their environments in Yangtze River system (2017–2021), Aquaculture and Fisheries (2023). https://doi.org/10.1016/j.aaf.2023.06.004.
[49] J.A. Darling, C.L. Jerde, A.J. Sepulveda, What do you mean by false positive? Environmental DNA 3 (5) (2021) 879–883.
[50] A. Baselga, C.D.L. Orme, betapart: an R package for the study of beta diversity, Methods Ecol. Evol. 3 (5) (2012) 808–812.
[51] M. Scriver, et al., Harnessing Decay Rates for Coastal Marine Biosecurity Applications: A Review of Environmental DNA and RNA Fate, Environmental DNA, 2023, pp. 1–13.
[52] T. Jo, et al., Warm Temperature and Alkaline Conditions Accelerate Environmental RNA Degradation, Environmental DNA, 2022.
[53] N.T. Marshall, H.A. Vanderploeg, S.R. Chaganti, Environmental (e)RNA advances the reliability of eDNA by predicting its age, Sci. Rep. 11 (1) (2021) 2769.

[54] Y. Inoue, et al., Environmental nucleic acid pollution: characterization of wastewater generating false positives in molecular ecological surveys, ACS ES&T Water 3 (3) (2023) 756−764.

[55] K. Kagzi, et al., Environmental RNA degrades more rapidly than environmental DNA across a broad range of pH conditions, Molecular Ecology Resources 22 (7) (2022) 2640−2650.

[56] K. Kagzi, et al., Assessing the Degradation of Environmental DNA and RNA Based on Genomic Origin in a Metabarcoding Context, Environmental DNA, 2023.

[57] J.L. Blanchard, et al., From bacteria to whales: using functional size spectra to model marine ecosystems, Trends Ecol. Evol. 32 (3) (2017) 174−186.

[58] A. Zaiko, et al., Assessing the performance and efficiency of environmental DNA/RNA capture methodologies under controlled experimental conditions, Methods Ecol. Evol. 13 (7) (2022) 1581−1594.

[59] R.C. Blackman, et al., Spatio-temporal patterns of multi-trophic biodiversity and food-web characteristics uncovered across a river catchment using environmental DNA, Commun. Biol. 5 (1) (2022) 259.

[60] M.I. Brandt, et al., An assessment of environmental metabarcoding protocols aiming at favoring contemporary biodiversity in inventories of deep-sea communities, Front. Mar. Sci. 7 (2020) 234.